Heparin and Other Glycosaminoglycans Stimulate the Formation of Amyloid Fibrils from α-Synuclein in Vitro†

Jeffrey A. Cohlberg,‡ Jie Li,‡ Vladimir N. Uversky, and Anthony L. Fink*

Department of Chemistry and Biochemistry, University of California, Santa Cruz, California 95064

Received August 23, 2001; Revised Manuscript Received November 6, 2001

ABSTRACT: Parkinson's disease is the second most common neurodegenerative disease and results from loss of dopaminergic neurons in the substantia nigra. The aggregation and fibrillation of α-synuclein have been implicated as a causative factor in the disease. Glycosaminoglycans (GAGs) are routinely found associated with amyloid deposits in most amyloidosis diseases, and there is evidence to support an active role of GAGs in amyloid fibril formation in some cases. In contrast to the extracellular amyloid deposits, the α-synuclein deposits in Lewy body diseases are intracellular, and thus it is less clear whether GAGs may be involved. To determine whether the presence of GAGs does affect the fibrillation of α-synuclein, the kinetics of fibril formation were investigated in the presence of a number of GAGs and other charged polymers. Certain GAGs (heparin, heparan sulfate) and other highly sulfated polymers (dextran sulfate) were found to significantly stimulate the formation of α-synuclein fibrils. Interestingly, the interaction of GAGs with α-synuclein is quite specific, since some GAGs, e.g., keratan sulfate, had negligible effect. Heparin not only increased the rate of fibrillation but also apparently increased the yield of fibrils. The molar ratio of heparin to α-synuclein and the incorporation of fluorescein-labeled heparin into the fibrils demonstrate that the heparin is integrated into the fibrils and is not just a catalyst for fibrillation. The apparent dissociation constant for heparin in stimulating α-synuclein fibrillation was 0.19 μM, indicating a strong affinity. Similar effects of heparin were observed with the A53T and A30P mutants of α-synuclein. Since there is some evidence that Lewy bodies may contain GAGs, these observations may be very relevant in the context of the etiology of Parkinson's disease.

There is abundant evidence that glycosaminoglycans (GAGs)[1] are involved in the formation of the amyloid deposits which are found in a variety of human diseases (reviewed in refs 1 and 2). Amyloid deposits are usually extracellular. Proteoglycans (PGs) containing heparan sulfate, chondroitin sulfate, keratan sulfate, and/or dermatan sulfate have been found in all amyloid deposits examined. A role for GAGs in amyloid formation is indicated by the fact that serum amyloid A (SAA) protein deposition is preceded by an increase in expression of the heparan sulfate PG perlecan in the extracellular matrix (*3*, *4*) and that in both SAA amyloidosis and Alzheimer Aβ amyloidosis heparan sulfate is deposited with a time course identical to that of the amyloid protein itself (*5*, *6*).

Evidence for the relation between GAGs and amyloid has also come from in vitro studies. GAGs and PGs stimulate in vitro formation of amyloid fibrils from the Alzheimer Aβ protein (*7*−*10*). Furthermore, PGs and GAGs bind directly to the Alzheimer amyloid precursor protein (APP) and to various forms of Aβ in vitro (*10*−*15*), with a much higher affinity for the fibrillar forms of these proteins than the soluble forms (*16*, *17*). Heparin and heparan sulfate also bind to the islet amyloid polypeptide amylin (*17*) and to SAA (*18*, *19*), and in both cases only amyloidogenic variants of the proteins exhibit binding. For both Aβ and SAA, GAG binding is accompanied by an increase in the content of β-sheet structure, a characteristic of amyloid fibrils (*2*, *10*, *18*, *19*). Finally, a number of studies have identified specific regions of APP and Aβ which appear to be involved in GAG binding (*11*, *14*, *20*−*22*).

In addition to being found in extracellular amyloid deposits, heparan sulfate is also associated with the intracellular neurofibrillary tangles (NFT), assembled from the microtubule-associated protein tau, which are found in Alzheimer patients (reviewed in refs *23* and *24*). Heparan sulfate enhances the phosphorylation of tau by various protein kinases in vitro (*25*−*30*) and directly stimulates NFT formation in vitro (*23*, *30*−*32*). Furthermore, heparan sulfate appears in nerve cells at the earliest stages of tau pathology prior to the appearance of NFTs (*23*). It has been proposed that leakage of heparan sulfate or heparan sulfate PGs into the cytoplasm of neurons could stimulate hyperphosphorylation of tau, followed by release of tau from microtubules and assembly into NFT (*23*).

In the present work we demonstrate a similar effect of GAGs and related compounds on the formation of amyloid fibrils from α-synuclein. α-Synuclein, a protein of 140 amino

† This research was supported by a grant from the National Institutes of Health (A.L.F.) and a sabbatical leave from California State University, Long Beach (J.A.C.).

* To whom correspondence should be addressed. Phone: (831) 459-2744. Fax: (831) 459-2935. E-mail: enzyme@cats.ucsc.edu.

‡ These authors contributed equally to this work.

[1] Abbreviations: Aβ, Alzheimer's β-amyloid peptide; APP, amyloid protein precursor; bFGF, basic fibroblast growth factor; EM, electron microscopy; GAG, glycosaminoglycan; NFT, neurofibrillary tangles; PG, proteoglycan; SAA, serum amyloid A; ThT, thioflavin T.

10.1021/bi011711s CCC: $22.00
Published on Web 01/11/2002

acids found in abundance in the presynaptic regions of neurons, is the principal component of Lewy bodies. These insoluble fibrous protein deposits are found in neurons of the substantia nigra in the brains of patients with Parkinson's disease and in the brain cortex in the Lewy body variant of Alzheimer's disease and dementia with Lewy bodies. Lewy bodies also appear to contain heparan sulfate PGs (*33*). α-Synuclein is also the major component of the glial cytoplasmic inclusions of multiple system atrophy, and a fragment of α-synuclein also has been identified as the non-Aβ component (NAC) of Alzheimer plaques. Two forms of familial Parkinson's disease are due to mutations in α-synuclein (reviewed in refs *34*−*36*).

The function of α-synuclein is unknown. The isolated protein lacks any organized secondary or tertiary structure (*37*). However, it acquires a high content of α-helix upon binding to membranes and phospholipid vesicles (*38*−*41*), and it may have a role in regulating synaptic vesicle formation (*42*). α-Synuclein has also been shown to have protein chaperone activity (*43*). It also binds to and inhibits phospholipase D (*44*). Other binding partners include the microtubule-associated proteins tau (*45*) and MAP-IB (*46*) and the protein synphilin-1 (*47*).

Incubation of recombinant α-synuclein for prolonged periods at 37 °C leads to the formation of typical amyloid fibrils with a morphology similar to those of fibrils isolated from Lewy bodies (*48*−*55*). Fibril formation is strongly accelerated by agitation (*56*), and the kinetics of fibril formation are highly dependent on pH and ionic strength (*57*). Fibril formation in vitro can be easily monitored by an increase in fluorescence of the dye thioflavin T (ThT) (*57*, *58*).

In this study we show that both the extent and rate of formation of amyloid fibrils from α-synuclein are greatly enhanced by heparin and certain other GAGs and charged polymers. We show that the fibrils formed from wild-type α-synuclein in the presence of heparin have some significant differences in morphology relative to those formed in its absence, although smaller differences in morphology were observed with the mutant α-synucleins. These results raise the possibility that GAGs may play a key role in the formation of Lewy bodies and in the etiology of Parkinson's disease and other diseases involving α-synuclein aggregates.

EXPERIMENTAL PROCEDURES

Materials. GAGs and other polymers used were as follows. Porcine intestinal heparin (grade I-A, mol wt 18000), *N*-acetylheparin (mol wt 18000), polyglutamic acid, sodium salt (P4636, mol wt 14300), polylysine hydrochloride (P2658, mol wt 16000), heparan sulfate from porcine intestinal mucosa (mol wt 7500), keratan sulfate from bovine cornea, chondroitin sulfate C (90% chondroitin-6-sulfate, 10% chondroitin-4-sulfate), chondroitin sulfate B (dermatan sulfate), dextran sulfate (D6924, mol wt 10,000), dextran (D9260, mol wt 10,000), salmon testes DNA, yeast tRNA, and baker's yeast RNA (R7125) were obtained from Sigma. Chondroitin sulfate A (90% chondroitin-4-sulfate, 10% chondroitin-6-sulfate) was from Calbiochem. Fluorescein-labeled heparin, containing 0.9 mol of fluorescein/mol of heparin, was obtained from Pierce. Thioflavin T was obtained from Sigma, St. Louis, MO. All other chemicals were of analytical grade from Fisher Chemicals or VWR Scientific.

Recombinant human α-synuclein was purified using the Impact system (New England Biolabs) as described previously (*57*). α-Synuclein fused to an intein containing a chitin-binding domain was adsorbed onto a chitin affinity column, and cleavage with dithiothreitol released free α-synuclein. The protein was eluted and dialyzed extensively against 10 mM Tris-HCl, 50 mM NaCl, and then water and then lyophilized in small aliquots. Lyophilized protein was dissolved immediately before use in 2 mM NaOH, the pH was adjusted to 10.7−11.3 with NaOH, and the protein was incubated for 10 min at room temperature (to dissolve any seeds) before the pH was readjusted to 8 with HCl. The protein concentration was determined by measuring the absorbance at 275 nm and using an extinction coefficient of 0.40 mg^{-1} cm^2. For most assays the solution was centrifuged at 13000 rpm for 15 min and the supernatant taken for the fibrillation assay.

Fibril Formation Assays. Assay solutions contained protein at a concentration of 0.25−1.0 mg/mL (18−70 μM) in 20 mM Tris-HCl and 0.1 M NaCl, pH 7.5 (fibrillation buffer) at room temperature, containing 10 or 20 μM ThT with GAGs or other additives as indicated. A volume of 75 or 100 μL of the mixture was pipetted into a well of a 96-well plate (white plastic, clear bottom), and a $^1/_8$th in. diameter Teflon sphere (McMaster-Carr, Los Angeles) was added. Each sample was run in triplicate or quadruplicate. The plates were sealed with Mylar plate sealers (Dynex). The plate was loaded into a fluorescence plate reader (Fluoroskan Ascent) and incubated at 37 °C with shaking at 300−600 rpm with a shaking diameter of 1 mm. The rate of fibrillation showed some dependence on the shaking speed, and a constant shaking speed was used for all samples within each experiment. The samples were shaken in order to speed the rate of fibril formation; agitation causes a very significant increase in the rate of fibrillation, due, we believe, to the hydrophobic nature of the air−water interface increasing the concentration of the critical partially folded intermediate. The fluorescence was measured at 15 min intervals with excitation at 450 nm and emission at 485 nm, with a sampling time of 40 ms. The data from replicate wells were averaged before plotting fluorescence vs time.

The data were fit to a sigmoidal equation (eq 1) using Sigmaplot:

$$F = (F_i + m_i t) + (F_f + m_f t)/\{1 + \exp[-(t - t_m)/\tau]\} \quad (1)$$

where F is the fluorescence intensity and t_m is the time to 50% of maximal fluorescence. The initial baseline during the lag time is described by $F_i + m_i t$. The final baseline after the growth phase has ended is described by $F_f + m_f t$. The apparent rate constant, k_{app}, for the growth of fibrils is given by $1/\tau$, the lag time is calculated as $t_m - 2\tau$, and the amplitude, amp, is given by $F_f - F_i$. Although eq 1 gave very good fits for the ThT kinetic profiles, the expression is strictly a simple empirical means of providing kinetic parameters for comparing rates of fibrillation from different samples and does not directly reflect the underlying complex kinetic scheme.

Fluorescence Measurements. In the experiments with fluorescent heparin, fluorescence was measured in a Fluoromax-II spectrophotometer (Spex, Instruments SA). Fluorescein spectra were obtained with an excitation wavelength

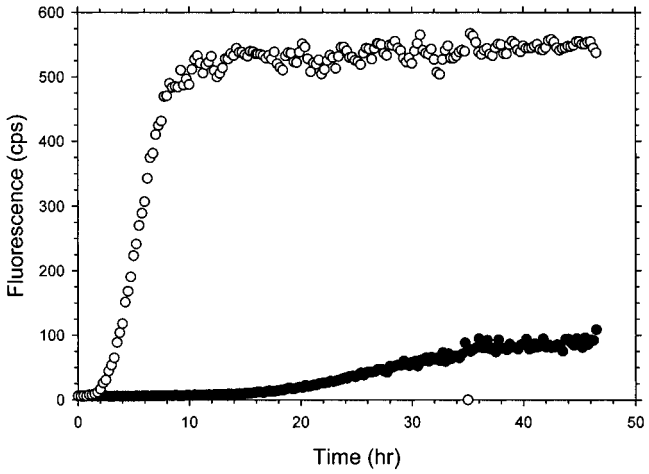

FIGURE 1: Heparin stimulates the formation of amyloid fibrils from α-synuclein. Fibrillation was monitored by the increase in fluorescence of thioflavin T, as described in Experimental Procedures, with 0.5 mg/mL α-synuclein. Key: open circles, 75 μg/mL heparin; closed circles, no heparin. The associated kinetic parameters are given in Table 1.

of 492 nm in a 250 μL cylindrical cuvette. To monitor fibril formation, 10 μL of each reaction mixture was diluted to 1 mL with 20 μM ThT, and the fluorescence was measured with an excitation wavelength of 450 nm and an emission wavelength of 482 nm. In the experiments to measure incorporation of fluorescein-labeled heparin into α-synuclein fibrils, 320 μL of fibrillation buffer containing 1.04 mg/mL (74 μM) α-synuclein and 5 μg/mL (0.28 μM) fluorescein−heparin was pipetted into two wells of a 96-well plate and incubated with agitation in the Fluoroskan Ascent plate reader overnight. The fibrils were recovered by pelleting for 30 min at 13000 rpm in a microcentrifuge. The first pellet was resuspended in 240 μL of fibrillation buffer and pelleted again. The second pellet was washed in a similar fashion with fibrillation buffer containing 1 M NaCl.

Electron Microscopy. Transmission electron micrographs were collected using a JEOL JEM-100B microscope operating with an accelerating voltage of 80 kV. Typical nominal magnifications ranged from 20000−50000×. Samples were deposited on Formvar-coated 300 mesh copper grids and negatively stained with 1% aqueous uranyl acetate.

RESULTS

Heparin Increases the Rate of Fibril Formation. Thioflavin T (ThT) fluorescence was used to follow the time course of fibril formation (*57*, *58*). This dye forms a complex with amyloid fibrils whose fluorescence intensity is proportional to the amount of fibrils present when the ThT concentration is held constant (*59*, *60*). These experiments used 20 μM ThT and protein concentrations up to 70 μM. Increasing the ThT concentration did not result in increased fluorescence, even at the highest protein concentrations. This indicated that the fluorescence was not limited by the ThT concentration, even though the protein was present in molar excess. Control experiments showed a linear increase in ThT fluorescence as a function of α-synuclein fibril concentration.

In the presence of 75 μg/mL heparin, both the rate and the extent of fibril formation increased. A typical result is shown in Figure 1 for an experiment at an α-synuclein concentration of 0.5 mg/mL. This corresponds to a protein concentration of 34.6 μM and a heparin polymer concentration of 4.2 μM or a monosaccharide residue concentration of approximately 260 μM. In the absence of heparin, the ThT fluorescence exhibited a sigmoidal time course, with a lag time of approximately 20 h, as reported previously (*57*). In the presence of heparin, the plateau fluorescence value was much higher, and the lag time was much shorter. The data were fit to eq 1 (see Experimental Procedures), and the results are tabulated in Table 1. For wild-type α-synuclein, heparin induced a 6-fold increase in the fluorescence signal for the plateau value (amp) relative to that in the absence of heparin. The rate constant for fibril growth, indicated by the value of $1/\tau$, increased 4-fold. The time to half-maximal fluorescence, t_m, was reduced 5-fold from 27.8 to 5.4 h, and the lag time was reduced 6-fold from 17.8 to 2.9 h.

Table 1: Kinetics of α-Synuclein Aggregation in the Presence and Absence of Heparin[a]

		amp (arbitrary units)	τ (h)	t_m (h)	lag time (h)
wild type	no heparin	87	4.99	27.8	17.8
	75 μg/mL heparin	535	1.25	5.4	2.9
A53T	no heparin	150	2.01	5.1	8.5
	75 μg/mL heparin	320	0.49	1.9	1.9
A30P	no heparin	80	6.44	25.0	22.5
	75 μg/mL heparin	210	0.81	5.0	3.4

[a] Derived from data fit to eq 1, as described in Experimental Procedures, where amp represents the total change in TFT signal, τ represents the time constant ($1/k$) for fibril growth, t_m is the time to the midpoint of the transition, and the lag time is the time at which the growth in fibrils becomes detectable. The errors in the kinetic parameters were ±10−15%.

When fibril formation was allowed to go to completion, as measured by the leveling off of the ThT signal, the subsequent addition of heparin led to small increases in fluorescence intensity, which eventually decreased to zero when added at longer time intervals (data not shown).

Effects of Different Glycosaminoglycans and Polymers. The effects of different GAGs and polymers on α-synuclein fibril formation were examined. Preliminary experiments (data not shown) were performed with each polymer concentration adjusted to give a monomer residue concentration of about 400 μM. Both heparan sulfate and *N*-acetylheparin gave strong stimulation, while keratan sulfate, chondroitin sulfate C, polyglutamate, polylysine, and RNA had little or no effect. In subsequent experiments, for all polymers other than heparin, *N*-acetylheparin, and heparan sulfate, a 10-fold higher monomer residue concentration of about 4 mM was used. The results of some of these experiments are shown in Figure 2. The various GAGs and polymers used, and the resulting kinetic parameters obtained from fitting the data to eq 1 are summarized in Table 2. The data for chondroitin sulfate A, RNA, tRNA, and DNA were omitted from the figure for clarity. The results show that *N*-acetylheparin and heparan sulfate were nearly as effective as heparin in increasing both the yield and rate of fibril formation. Chondroitin sulfate A and chondroitin sulfate B (dermatan sulfate) had a much smaller effect, even at the higher concentrations, and very little effect was seen with chondroitin sulfate C or keratan sulfate. Thus the magnitude of the effect depended strongly on which GAG was used in the assay, with heparin and heparan sulfate showing the

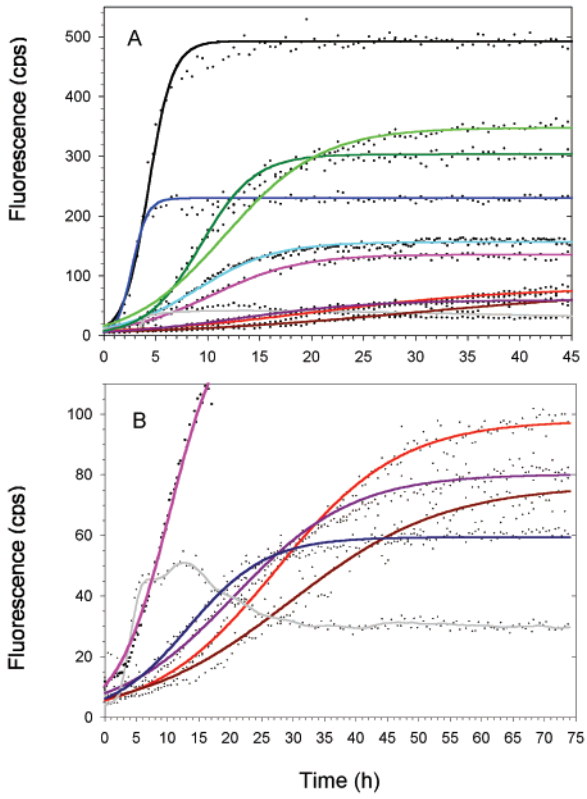

FIGURE 2: Various GAGs and polymers have different effects on α-synuclein fibrillation. Assays were performed as in Figure 1. Panel B is an expansion of the ordinate for those samples with the lowest ThT signals. The solid lines represent the fit of the data to eq 1, except for polylysine (gray curve). In order of decreasing intensity the curves are as follows: black, heparin; light green, heparan sulfate; dark green, *N*-acetylheparin; blue, 1.04 mg/mL dextran sulfate; cyan, chondroitin sulfate B; pink, polyglutamic acid; red, no additions; purple, keratan sulfate; brown, dextran; dark blue, chondroitin sulfate C; gray, polylysine.

Table 2: Effect of Glycosaminoglycans and Other Additives on α-Synuclein Aggregation[a]

	concentration					
additive	μg/mL	monomer (mM)	polymer (μM)	amp	τ (h)	t_m (h)
none				106	11.1	26.0
heparin	75	0.26	4.2	541	1.24	4.0
heparan sulfate	99	0.40	13	528	4.87	9.1
N-acetylheparin	84	0.31	4.7	300	2.43	8.7
chondroitin sulfate A	960	4.0	50	184	14.3	24.0
chondroitin sulfate B	960	4.0	50	161	5.6	18.0
chondroitin sulfate C	960	4.0	50	76	4.86	12.0
keratan sulfate	930	4.0	80	93	10.9	16.6
polylysine	660	4.0	41	41	0.41	4.0
polyglutamic acid	520	4.0	36	130	3.79	9.9
dextran sulfate	1040	3.7	104	202	0.51	2.6
dextran	720	1.4	72	61	7.9	31.5
tRNA	1330	4.0	54	105	9.9	15.9
total RNA	1330	4.0		112	12.7	21.7
DNA	100	0.3		106	10.4	22.3

[a] α-Synuclein fibrillation assays were performed as described in Experimental Procedures with a protein concentration of 0.5 mg/mL; the data were analyzed with eq 1. The errors in the kinetics parameters were ±10−15%. For each GAG at least two independent experiments with three to four wells were averaged for each sample.

strongest stimulation. The absence of any effect by keratan sulfate, RNA, and DNA indicates that the stimulation is not simply a nonspecific consequence of the presence of polyanions.

Charged polymers other than GAGs were also tested for their effects on α-synuclein aggregation. Dextran sulfate at a concentration of 1.04 mg/mL reproducibly gave faster fibril formation than heparin (at 75 μg/mL), albeit at a somewhat reduced yield, while dextran had a slight inhibitory effect. [A less dramatic stimulation (data not shown) was observed when dextran sulfate was used at a concentration comparable to that of heparin.] This demonstrates that the presence of charged groups is essential for the stimulatory effect. Polyglutamic acid also gave substantial stimulation, but considerably less than heparin. Polylysine reproducibly gave an initial burst of fluorescence intensity, which then decayed slowly as time proceeded. This was not due to dye binding by polylysine, since control mixtures with polylysine in the absence of α-synuclein gave no fluorescence above baseline values. Thus charged polymers other than polysaccharides are capable of stimulating α-synuclein fibrillation.

The presence of DNA or RNA had negligible effect on α-synuclein fibrillation relative to that for the control. RNA (in the absence of α-synuclein) showed an enhancement of ThT fluorescence, which decayed slowly with time; therefore, the data for samples containing α-synuclein and RNA were corrected by subtracting the data for the RNA controls lacking α-synuclein.

Dependence of Kinetics of Fibril Formation on Heparin Concentration. The dependence of the kinetics of fibrillation on heparin concentration is shown in Figure 3A. For this experiment the α-synuclein concentration was 0.3 mg/mL, compared to 0.5 mg/mL in Figures 1 and 2, and the shaking rate was reduced to 300 rpm instead of 600 rpm. The addition of increasing concentrations of heparin led to a reduction of the lag and a progressive increase in the magnitude of the plateau fluorescence value. In Figure 3B, the plateau fluorescence is plotted vs heparin concentration and fitted to the equation for a hyperbolic saturation curve, $y = y_0 + ax/(b + x)$, in which x is heparin concentration and b is the heparin concentration needed for half-maximal fluorescence enhancement, or the apparent heparin dissociation constant. The data are well fit by a curve with $b = 3.4$ μg/mL, which is a heparin polymer concentration of 0.19 μM or (assuming that the repeat unit of heparin is a disaccharide of L-iduronic acid-2-sulfate and *N*-sulfo-D-glucosamine-6-sulfate) a monosaccharide residue concentration of 10 μM.

Heparin Is Incorporated into Fibrils. In stimulating fibril formation, heparin could be incorporated into amyloid fibrils, or it could be acting in a catalytic fashion. To distinguish between these possibilities, a fibrillation experiment was conducted in the presence of fluorescein-labeled heparin, containing 0.9 mol of fluorescein/mol of heparin. The reaction mixture contained α-synuclein at a concentration of 1.0 mg/mL (74 μM) and fluorescein−heparin at a concentration of 5.0 μg/mL (0.28 μM) in a volume of 320 μL. The fluorescence spectra of the samples containing heparin and protein taken immediately after mixing were identical to the spectra containing heparin alone at the same concentration, with a fluorescence maximum at 511 nm (Figure 4).

The sample was pipetted into two wells of a 96-well plate and incubated with agitation in the Fluoroskan Ascent plate reader overnight. Samples were withdrawn at 19 and 22 h,

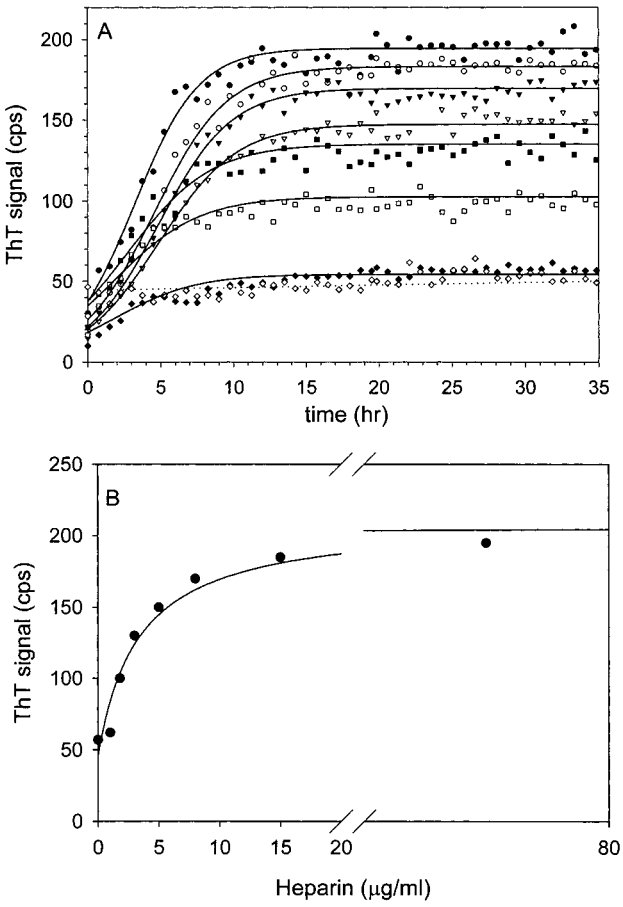

FIGURE 3: Effect of heparin concentration on α-synuclein fibrillation kinetics. (A) Assays were performed as in Figure 1, with heparin concentrations of 75 (filled circles), 15 (open circles), 8 (filled inverted triangles), 5 (open inverted triangles), 3 (filled squares), 1.8 (open squares), 1 (filled diamonds), and 0 (open diamonds) μg/mL. The solid lines are fits to eq 1. (B) Dependence of plateau fluorescence on heparin concentration. The data were taken from the 35 h fluorescence values in panel A. The solid line is a fit of the data to the equation $y = 46 + 165/(x + 3.4)$.

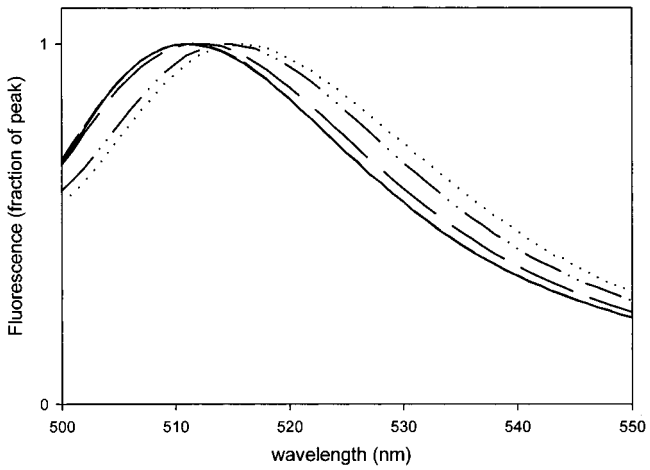

FIGURE 4: Emission spectra of samples containing fluorescein-labeled heparin. The preparation of samples is described in the legend to Table 3. Spectra were obtained as described in the text. Each spectrum was normalized by dividing the cps at each wavelength by the cps at the peak. The actual cps values are given in Table 3. Key: solid line, fluorescein−heparin with no protein; short dashes, protein samples before incubation (these two spectra are superimposed); long dashes, protein samples after incubation; dashes and dots, initial pellet; dots, final pellet.

Table 3: Incorporation of Fluorescein-Labeled Heparin into α-Synuclein Fibrils[a]

fraction	peak fluorescence (total cps)	λ_{max} (nm)
fluorescein−heparin plus protein, initial reaction mixture	1 537 392	511
final reaction mixture	1 294 500	511−512
first pellet	349 813 (27%)	514−515
first supernatant	968 696 (75%)	
second supernatant	46 376 (14% of first pellet)	
third (high-salt) supernatant	94 682 (28% of first pellet)	
final pellet	190 643 (57% of first pellet)	516

[a] Fluorescein emission spectra were obtained as described in Experimental Procedures.

and measurements of ThT fluorescence confirmed that fibrils had formed and that fibrillation was complete. Also, SDS gel electrophoresis of the pellet and supernatant revealed that nearly all of the protein was contained in the pellet (data not shown). A sample was examined by electron microscopy, revealing fibrils of normal morphology.

The fibrils were then recovered by pelleting, and about 27% of the total fluorescence-labeled heparin was recovered in the pellet (Table 3). The pellet was then washed, first with fibrillation buffer and then with fibrillation buffer containing 1 M NaCl. Fluorescence spectra of all supernatants and pellets were obtained, and the results are summarized in Figure 4 and Table 3. The data in the table demonstrate that the fluorescein-labeled heparin remained associated with the pelleted protein. Even after successive washings in both low- and high-salt buffer, 57% of the fluorescein originally pelleted was recovered in the final protein pellet (the decreased value is attributed predominantly to loss of fibrils in the washing procedure; see below).

The spectra also revealed that fibril assembly caused a red shift in the fluorescein emission spectrum. Gradual removal of unbound fluorescein during repeated pelleting produced a further red shift, with the initial pellet showing an emission maximum at 514−515 nm and the final pellet having a maximum at 516 nm (compared to 510 nm in the free compound). Control experiments in which fibrils grown in the absence of heparin were washed with buffer in a similar manner also showed some loss of α-synuclein from the fibrils, indicating that α-synuclein fibrils dissolve, at least to some extent, at neutral pH. Thus the figure of 57% should be taken as a lower limit of the fraction of the heparin in the initial pellet that was associated with protein fibrils. Thus the decrease in the total fluorescence was due mainly to the removal of unbound fluorescence label, but there was also some contribution from resolubilization of pellets during the washing procedure. The sample was also centrifuged for 30 min at 13000 rpm in a microcentrifuge. SDS gel electrophoresis of the pellet and supernatant revealed that nearly all of the protein was contained in the pellet (data not shown).

Heparin Stimulates the Aggregation of Mutant α-Synucleins Associated with Parkinson's Disease. Two point mutations in α-synuclein are associated with rare familial early-onset Parkinson's disease, A53T and A30P. Both mutants aggregate more rapidly than the wild type, although fibril formation is more rapid with the A53T mutant and slower with the A30P mutant (*48*, *49*, *51*, *54*, *55*, *58*, *71*). As with the wild-type protein, heparin dramatically stimu-

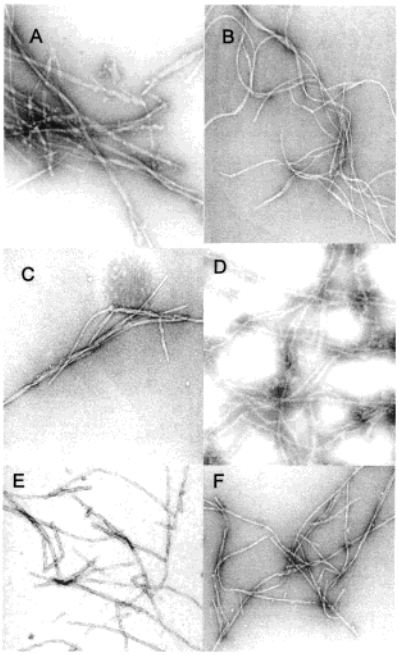

FIGURE 5: Electron microscope images of fibrils formed from α-synuclein and its mutants in the presence and absence of heparin. Panels A, C, and E are in the absence of heparin; panels B, D, and F were grown in the presence of 75 μg/mL heparin. Panels A and B are wild-type α-synuclein, panels C and D are A53T, and panels E and F are A30P. The panels are approximately 500 nm wide.

lated fibril formation with the mutant α-synucleins (Table 1). There were modest differences in the kinetics of the heparin-stimulated fibrillation reactions, with the kinetics being fastest with wild-type α-synuclein and the A53T variant and slowest with A30P. From measuring the kinetics of fibril formation as a function of heparin concentration it is clear that there are significant differences in affinity of the three proteins for heparin. Thus, the apparent dissociation constants were 0.6 μM for A30P and 0.03 μM for A53T (data not shown), in contrast to the value of 0.19 μM for wild-type α-synuclein.

Effect of Heparin on Fibril Morphology. Electron microscope images of amyloid fibrils formed from α-synuclein in the absence and presence of 75 μg/mL heparin are shown in Figure 5. In the absence of heparin (Figure 5A), long needlelike fibrils were observed with a diameter of 6−12 nm for wild-type α-synuclein (the thicker fibrils appeared to arise from interaction of thinner ones). In the presence of heparin (Figure 5B), the fibrils appeared thinner, with a more uniform diameter of 6 nm, much longer, and many fibrils were curved (Figure 5B).

The effects of heparin on the morphology of fibrils grown from the A30P and A53T mutants of α-synuclein were also examined. As shown in Figure 5C,D (A30P) and 5E,F (A53T), there were smaller differences between the fibrils of the mutants in the presence and absence of heparin. Again, curvature was seen more commonly in the presence of heparin, especially with the A30P α-synuclein, and the fibrils in the presence of heparin tended to be thinner. This probably arises from the fact that lateral aggregation of fibrils appears to occur to a greater extent in the absence of heparin.

DISCUSSION

The data presented here show strong stimulation of α-synuclein aggregation into amyloid fibrils by glycosaminoglycans, particularly heparin and heparan sulfate. A similar stimulation of amyloid formation has been observed for several other proteins which form amyloid, as noted in the introduction. These results suggest that GAGs or proteoglycans could play a role in the formation of the amyloid deposits of α-synuclein found in Lewy bodies. The finding that Lewy bodies contain heparinase-sensitive binding sites for basic fibroblast growth factor (bFGF) indicates that heparan sulfate PGs are constituents of Lewy bodies (*33*). The bFGF binding was observed only at the periphery of Lewy bodies, and this occurred with only a fraction of Lewy bodies in Parkinson's disease and not at all with the inclusions from diffuse Lewy body disease. Further work with different methods for detecting GAGs would be useful in more extensively characterizing the extent of GAG association with Lewy bodies.

The relevance of these observations to the formation of fibrillar deposits of α-synuclein in Lewy bodies is uncertain at this time. In the cases of the Alzheimer Aβ protein, serum amyloid A protein, and amylin, the amyloid deposits are extracellular, and a direct interaction of extracellular proteoglycans with amyloidogenic proteins provides a simple in vivo mechanism for the stimulation of fibril formation by GAGs. In the case of the neurofibrillary tangles of the protein tau which occur in Alzheimer's disease, the occurrence of heparan sulfate in the cytoplasm of affected nerve cells prior to the appearance of tangles raises the possibility that tangle formation is triggered by the leakage of heparan sulfate PGs into the cytoplasm of neurons during the early stages of cell degeneration. It is conceivable that similar leakage of GAGs or PGs into neurons could provide the trigger for formation of α-synuclein aggregates in Parkinson's disease and other Lewy body diseases. The presence of chondroitin sulfates within axon terminals has also been reported (*70*).

The strength of the effect of GAGs and other polymers on fibril formation varies with the particular polymer used. Similar variation was found with studies on other amyloidogenic proteins. In the case of the Alzheimer Aβ protein, chondroitin-6-sulfate was most effective in stimulating aggregation, with lesser effects seen with dermatan sulfate and chondroitin-4-sulfate, followed by (in decreasing order) heparan sulfate, keratan sulfate, and heparin (*7*). For tau aggregation, the strongest effect was seen with heparin, dextran sulfate, and pentosan sulfate, followed by heparan sulfate and RNA, with weak stimulation by dermatan sulfate and chondroitin sulfate, and no stimulation by keratan sulfate, hyaluronic acid, dextran, and polyglutamic acid (*23*). Another study with tau did report stimulation of assembly by polyglutamic acid; in this case heparin had the strongest effect, followed by RNA and then by polyglutamic acid (*32*).

Our results with α-synuclein show that heparin and dextran sulfate had the strongest effect, with a slightly weaker effect with heparan sulfate, weaker effects with polyglutamic acid, polylysine, chondroitin-4-sulfate, and dermatan sulfate, and little or no effect with chondroitin-6-sulfate, keratan sulfate, DNA, and RNA, and inhibition by dextran. These results are similar to those seen with tau, with the notable exception that we observed no stimulation of amyloid formation by RNA, while RNA strongly stimulated tau aggregation. It is interesting to note that RNA has been found associated with both the Aβ plaques and the tau neurofibrillary tangles

associated with Alzheimer's disease but could not be detected in Lewy bodies (*61*, *62*). This correlates with the different effects of RNA on in vitro fibril formation for tau and α-synuclein.

Heparin binding sites on a variety of proteins have been characterized and are invariably shown to contain clusters of basic amino acid residues capable of binding to the negatively charged heparin polymer (*63*). In the case of a number of proteins and polypeptides which are induced to form β-structure by heparin, the heparin binding sequences consist of alternating basic and nonbasic residues (*63*). These include apolipoprotein E (*64*), an alternating copolymer of lysine and tyrosine (*65*), and one of the heparin binding domains of the Alzheimer amyloid precursor protein (*14*, *20*). Formation of a β-sheet structure would cause the alternating basic side chains to point in the same direction perpendicular to the plane of the sheet, and binding to a polyanion might stabilize the β-structure. The N-terminal region of α-synuclein contains multiple repeats of the consensus sequence KTKEGV, and pairs of lysine residues spaced two residues apart occur at positions 10/12, 21/23, 33/35, 42/44, and 58/60 (*67*, *68*). It is likely that this region of α-synuclein constitutes the GAG binding region and that it is the transition of the protein from an unstructured state to a β-sheet conformation which creates a site for GAG binding. This is an interesting possibility, because it has been shown that the repeat sequences of α-synuclein are predicted to form amphiphilic helices, and when α-synuclein binds to lipids, α-helical structure is observed. We have recently shown that α-synuclein forms a partially folded conformation that is enriched in β-structure (*57*), so it is possible that this intermediate is the conformation that binds to heparin.

The experiments with fluorescein-labeled heparin show that heparin pellets with α-synuclein fibrils on centrifugation and remains tightly associated with the fibrils during repeated washing at both high- and low-salt concentrations. The results further demonstrate that fibril assembly is accompanied by a red shift of fluorescein fluorescence emission. These data demonstrate that heparin is incorporated into the fibrils and rule out a purely catalytic effect of heparin on fibril formation. The fluorescence red shift indicates that the fluorescein fluorophores are in a more polar environment in the fibrils than in free solution. This is consistent with the idea that heparin binds to sites on the protein with a high content of amino acid residues with positively charged side chains.

The origin of the more curved fibril morphology, especially for wild-type α-synuclein fibrils grown in the presence of heparin, is unclear but could suggest that heparin is acting as a template for fibrillation. In experiments with an α-synuclein concentration of 35 μM, half-maximal ThT fluorescence enhancement was observed at a heparin polymer concentration of 0.19 μM or a monosaccharide residue concentration of 10 μM. This corresponds to a 200:1 ratio of polypeptide chain to heparin polymer or a 3.5:1 ratio of polypeptide chain to monosaccharide unit. One possible interpretation of these ratios is that the form of α-synuclein that binds heparin is oligomeric rather than monomeric and that many such species can be bound to a single heparin polymer, which consists of about 60 monosaccharide units. One possibility for this oligomeric species would be the fibrillation nucleus. The sigmoidal kinetics of fibril formation are often attributed to a nucleated polymerization mechanism, in which the lag corresponds to formation of the nucleus and the exponential increase corresponds to fibril growth (*48*, *57*, *58*, *68*, *69*). It is interesting to note that heparin affects both the nucleation and fibril growth stages of the process. However, it is also possible that heparin binds to a specific population of α-synuclein, perhaps a minority conformation, which then seeds fibril formation.

In all cases, the presence of heparin caused a marked increase in the final ThT fluorescence signal. There are two possible types of explanation for this effect: either there is an increase in the amount of fibrils when heparin is present or the presence of the heparin, directly or indirectly, affects the intensity of the ThT signal. In fact, an increase in the yield of fibrils in the presence of heparin was consistent with an increased yield of fibrils by electron microscopy; however, the increase appeared to be significantly less than anticipated on the basis of the severalfold increase in ThT intensity. This raises two questions: How could heparin affect the yield of fibrils, and what else could account for the increased signal? One possible explanation of the former is that there is a branched pathway for α-synuclein aggregation, with one branch leading to fibrils and the other to soluble oligomers, and the presence of heparin shifts the partitioning to favor fibrils (*71*).

However, a second class of phenomena could lead to an increased fluorescence signal, even without an increase in the number of fibrils, due to effects on the ThT binding and signal. For example, lateral aggregation or clumping of α-synuclein fibrils was often observed in EM and atomic force microscopy images, and such clumping could decrease the number of available ThT sites (in the absence of heparin). Also, the presence of heparin in the fibril could increase the ThT signal either by increasing the amount of ThT bound or by a local environmental effect on the ThT fluorescence emission. This could reflect somewhat different fibril morphologies in the presence and absence of heparin. [We note that filaments of the protein tau showed a 5-fold greater ThT fluorescence when formed in the presence of heparin than in the presence of polyglutamic acid (*32*)]. Heparin and heparan sulfate differ structurally in that the latter is less negatively charged and has fewer sulfate groups; since the ThT signal for heparan sulfate was less than that for heparin and even less for chondroitin and keratan sulfates, which have even fewer negatively charged groups, there appears to be a loose correlation between ThT intensity and charge density on the polymer. Similarly, in terms of the effect on the kinetics of fibrillation, the more highly charged polymers were more effective in accelerating the rates of fibril formation, leading to a correlation between increased kinetics of fibril formation and increased final ThT signal. Further work is needed to determine the relative importance of these two types of contributions to the ThT fluorescence intensity. The effects of polylysine are interesting on two counts: it has the opposite charge to the other polymers yet enhances fibrillation, and it leads to complex fibrillation kinetics as monitored by ThT. The data suggest a rapid formation of fibrils followed by a slower decrease in ThT-positive material. It is possible that the positively charged polylysine facilitates lateral aggregation of α-synuclein fibrils so as to decrease the number of ThT sites available to the dye, leading to the observed decrease at later times.

The effect of heparin on the kinetics of fibrillation of the mutant α-synucleins suggests that heparin interacts at an early stage of aggregation, prior to fibrillation. This is based on the observation that in the absence of heparin A30P α-synuclein forms soluble aggregates rapidly but forms fibrils more slowly than wild type. The A53T mutant, on the other hand, forms fibrils more rapidly than wild type. The data in Table 1 indicate that heparin causes A30P to form fibrils more rapidly than wild type, thus suggesting that heparin interacts with a normally transient soluble oligomer, which, in the case of A30P, is longer lived in the absence of heparin.

The results reported here raise the interesting possibility that proteoglycans or glycosaminoglycans could be directly involved in the etiology of Parkinson's disease and related α-synucleinopathies. For example, if heparin or a related GAG were present in a neuron, perhaps through a defect in endocytosis, it could come in contact with α-synuclein. Our data indicate that, at the high concentrations of α-synuclein anticipated in nerve terminals, relatively small amounts of GAG could cause a dramatic increase in the rate of α-synuclein fibrillation.

REFERENCES

1. Kisilevsky, R. (2000) Review: amyloidogenesis-unquestioned answers and unanswered questions, *J. Struct. Biol. 130*, 99−108.
2. McLaurin, J., Yang, D., Yip, C. M., and Fraser, P. E. (2000) Review: modulating factors in amyloid-beta fibril formation, *J. Struct. Biol. 130*, 259−270.
3. Ailles, L., Kisilevsky, R., and Young, I. D. (1993) Induction of perlecan gene expression precedes amyloid formation during experimental murine AA amyloidogenesis, *Lab. Invest. 69*, 443−448.
4. Woodrow, S. I., Stewart, R. J., Kisilevsky, R., Gore, J., and Young, I. D. (1999) Experimental AA amyloidogenesis is associated with differential expression of extracellular matrix genes, *Amyloid 6*, 22−30.
5. Lyon, A. W., Narindrasorasak, S., Young, I. D., Anastassiades, T., Couchman, J. R., McCarthy, K. J., and Kisilevsky, R. (1991) Co-deposition of basement membrane components during the induction of murine splenic AA amyloid, *Lab. Invest. 64*, 785−790.
6. Snow, A. D., Kisilevsky, R., Stephens, C., and Anastassiades, T. (1987) Characterization of tissue and plasma glycosaminoglycans during experimental AA amyloidosis and acute inflammation. Qualitative and quantitative analysis, *Lab. Invest. 56*, 665−675.
7. Castillo, G. M., Lukito, W., Wight, T. N., and Snow, A. D. (1999) The sulfate moieties of glycosaminoglycans are critical for the enhancement of beta-amyloid protein fibril formation, *J. Neurochem. 72*, 1681−1687.
8. Castillo, G. M., Ngo, C., Cummings, J., Wight, T. N., and Snow, A. D. (1997) Perlecan binds to the beta-amyloid proteins (A beta) of Alzheimer's disease, accelerates A beta fibril formation, and maintains A beta fibril stability, *J. Neurochem. 69*, 2452−2465.
9. Cotman, S. L., Halfter, W., and Cole, G. J. (2000) Agrin binds to beta-amyloid (Abeta), accelerates abeta fibril formation, and is localized to Abeta deposits in Alzheimer's disease brain, *Mol. Cell. Neurosci. 15*, 183−198.
10. McLaurin, J., Franklin, T., Zhang, X., Deng, J., and Fraser, P. E. (1999) Interactions of Alzheimer amyloid-beta peptides with glycosaminoglycans: effects on fibril nucleation and growth, *Eur. J. Biochem. 266*, 1101−1110.
11. Brunden, K. R., Richter-Cook, N. J., Chaturvedi, N., and Frederickson, R. C. (1993) pH-dependent binding of synthetic beta-amyloid peptides to glycosaminoglycans, *J. Neurochem. 61*, 2147−2154.
12. Buee, L., Ding, W., Anderson, J. P., Narindrasorasak, S., Kisilevsky, R., Boyle, N. J., Robakis, N. K., Delacourte, A., Greenberg, B., and Fillit, H. M. (1993) Binding of vascular heparan sulfate proteoglycan to Alzheimer's amyloid precursor protein is mediated in part by the N-terminal region of A4 peptide, *Brain Res. 627*, 199−204.
13. Buee, L., Ding, W., Delacourte, A., and Fillit, H. (1993) Binding of secreted human neuroblastoma proteoglycans to the Alzheimer's amyloid A4 peptide, *Brain Res. 601*, 154−163.
14. Multhaup, G. (1994) Identification and regulation of the high affinity binding site of the Alzheimer's disease amyloid protein precursor (APP) to glycosaminoglycans, *Biochimie 76*, 304−311.
15. Snow, A. D., Kinsella, M. G., Parks, E., Sekiguchi, R. T., Miller, J. D., Kimata, K., and Wight, T. N. (1995) Differential binding of vascular cell-derived proteoglycans (perlecan, biglycan, decorin, and versican) to the beta-amyloid protein of Alzheimer's disease, *Arch. Biochem. Biophys. 320*, 84−95.
16. Gupta-Bansal, R., Frederickson, R. C., and Brunden, K. R. (1995) Proteoglycan-mediated inhibition of A beta proteolysis. A potential cause of senile plaque accumulation, *J. Biol. Chem. 270*, 18666−18671.
17. Watson, D. J., Lander, A. D., and Selkoe, D. J. (1997) Heparin-binding properties of the amyloidogenic peptides Abeta and amylin. Dependence on aggregation state and inhibition by Congo red, *J. Biol. Chem. 272*, 31617−31624.
18. de Beer, M. C., de Beer, F. C., McCubbin, W. D., Kay, C. M., and Kindy, M. S. (1993) Structural prerequisites for serum amyloid A fibril formation, *J. Biol. Chem. 268*, 20606−20612.
19. McCubbin, W. D., Kay, C. M., Narindrasorasak, S., and Kisilevsky, R. (1988) Circular-dichroism studies on two murine serum amyloid A proteins, *Biochem. J. 256*, 775−783.
20. Mok, S. S., Sberna, G., Heffernan, D., Cappai, R., Galatis, D., Clarris, H. J., Sawyer, W. H., Beyreuther, K., Masters, C. L., and Small, D. H. (1997) Expression and analysis of heparin-binding regions of the amyloid precursor protein of Alzheimer's disease, *FEBS Lett. 415*, 303−307.
21. Clarris, H. J., Cappai, R., Heffernan, D., Beyreuther, K., Masters, C. L., and Small, D. H. (1997) Identification of heparin-binding domains in the amyloid precursor protein of Alzheimer's disease by deletion mutagenesis and peptide mapping, *J. Neurochem. 68*, 1164−1172.
22. McLaurin, J., and Fraser, P. E. (2000) Effect of amino acid substitutions on Alzheimer's amyloid-beta peptide-glycosaminoglycan interactions, *Eur. J. Biochem. 267*, 6353−6361.
23. Goedert, M., Jakes, R., Spillantini, M. G., Hasegawa, M., Smith, M. J., and Crowther, R. A. (1996) Assembly of microtubule-associated protein tau into Alzheimer-like filaments induced by sulphated glycosaminoglycans, *Nature 383*, 550−553.
24. Goedert, M. (1999) Filamentous nerve cell inclusions in neurodegenerative diseases: tauopathies and alpha-synucleinopathies, *Philos. Trans. R. Soc. London, Ser. B 354*, 1101−1118.
25. Mawal-Dewan, M., Sen, P. C., Abdel-Ghany, M., Shalloway, D., and Racker, E. (1992) Phosphorylation of tau protein by purified p34cdc28 and a related protein kinase from neurofilaments, *J. Biol. Chem. 267*, 19705−19709.
26. Brandt, R., Lee, G., Teplow, D. B., Shalloway, D., and Abdel-Ghany, M. (1994) Differential effect of phosphorylation and substrate modulation on tau's ability to promote microtubule growth and nucleation, *J. Biol. Chem. 269*, 11776−11782.
27. Yang, S. D., Yu, J. S., Shiah, S. G., and Huang, J. J. (1994) Protein kinase FA/glycogen synthase kinase-3 alpha after heparin potentiation phosphorylates tau on sites abnormally phosphorylated in Alzheimer's disease brain, *J. Neurochem. 63*, 1416−1425.
28. Hasegawa, M., Jakes, R., Crowther, R. A., Lee, V. M., Ihara, Y., and Goedert, M. (1996) Characterization of mAb AP422, a novel phosphorylation-dependent monoclonal antibody against tau protein, *FEBS Lett. 384*, 25−30.

29. Goedert, M., Hasegawa, M., Jakes, R., Lawler, S., Cuenda, A., and Cohen, P. (1997) Phosphorylation of microtubule-associated protein tau by stress-activated protein kinases, *FEBS Lett. 409*, 57−62.
30. Hasegawa, M., Crowther, R. A., Jakes, R., and Goedert, M. (1997) Alzheimer-like changes in microtubule-associated protein Tau induced by sulfated glycosaminoglycans. Inhibition of microtubule binding, stimulation of phosphorylation, and filament assembly depend on the degree of sulfation, *J. Biol. Chem. 272*, 33118−33124.
31. Perez, M., Valpuesta, J. M., Medina, M., Montejo de Garcini, E., and Avila, J. (1996) Polymerization of tau into filaments in the presence of heparin: the minimal sequence required for tau-tau interaction, *J. Neurochem. 67*, 1183−1190.
32. Friedhoff, P., Schneider, A., Mandelkow, E. M., and Mandelkow, E. (1998) Rapid assembly of Alzheimer-like paired helical filaments from microtubule-associated protein tau monitored by fluorescence in solution, *Biochemistry 37*, 10223−10230.
33. Perry, G., Richey, P., Siedlak, S. L., Galloway, P., Kawai, M., and Cras, P. (1992) Basic fibroblast growth factor binds to filamentous inclusions of neurodegenerative diseases, *Brain Res. 579*, 350−352.
34. Trojanowski, J. Q., Goedert, M., Iwatsubo, T., and Lee, V. M. (1998) Fatal attractions: abnormal protein aggregation and neuron death in Parkinson's disease and Lewy body dementia, *Cell Death Differ. 5*, 832−837.
35. Hashimoto, M., and Masliah, E. (1999) Alpha-synuclein in Lewy body disease and Alzheimer's disease, *Brain Pathol. 9*, 707−720.
36. Schulz, J. B., and Dichgans, J. (1999) Molecular pathogenesis of movement disorders: are protein aggregates a common link in neuronal degeneration?, *Curr. Opin. Neurol. 12*, 433−439.
37. Weinreb, P. H., Zhen, W., Poon, A. W., Conway, K. A., and Lansbury, P. T., Jr. (1996) NACP, a protein implicated in Alzheimer's disease and learning, is natively unfolded, *Biochemistry 35*, 13709−13715.
38. Davidson, W. S., Jonas, A., Clayton, D. F., and George, J. M. (1998) Stabilization of alpha-synuclein secondary structure upon binding to synthetic membranes, *J. Biol. Chem. 273*, 9443−9449.
39. Jensen, P. H., Nielsen, M. S., Jakes, R., Dotti, C. G., and Goedert, M. (1998) Binding of alpha-synuclein to brain vesicles is abolished by familial Parkinson's disease mutation, *J. Biol. Chem. 273*, 26292−26294.
40. Jo, E., McLaurin, J., Yip, C. M., St George-Hyslop, P., and Fraser, P. E. (2000) alpha-synuclein membrane interactions and lipid specificity, *J. Biol. Chem. 275*, 34328−34334.
41. Perrin, R. J., Woods, W. S., Clayton, D. F., and George, J. M. (2000) Interaction of human alpha-synuclein and Parkinson's disease variants with phospholipids. Structural analysis using site-directed mutagenesis, *J. Biol. Chem. 275*, 34393−34398.
42. Murphy, D. D., Rueter, S. M., Trojanowski, J. Q., and Lee, V. M. (2000) Synucleins are developmentally expressed, and alpha-synuclein regulates the size of the presynaptic vesicular pool in primary hippocampal neurons, *J. Neurosci. 20*, 3214−3220.
43. Souza, J. M., Giasson, B. I., Lee, V. M., and Ischiropoulos, H. (2000) Chaperone-like activity of synucleins, *FEBS Lett. 474*, 116−119.
44. Jenco, J. M., Rawlingson, A., Daniels, B., and Morris, A. J. (1998) Regulation of phospholipase D2: selective inhibition of mammalian phospholipase D isoenzymes by alpha- and beta-synucleins, *Biochemistry 37*, 4901−4909.
45. Jensen, P. H., Hager, H., Nielsen, M. S., Hojrup, P., Gliemann, J., and Jakes, R. (1999) Alpha-synuclein binds to Tau and stimulates the protein kinase A-catalyzed tau phosphorylation of serine residues 262 and 356, *J. Biol. Chem. 274*, 25481−25489.
46. Jensen, P. H., Islam, K., Kenney, J., Nielsen, M. S., Power, J., and Gai, W. P. (2000) Microtubule-associated protein 1B is a component of cortical Lewy bodies and binds alpha-synuclein filaments, *J. Biol. Chem. 275*, 21500−21507.
47. Engelender, S., Kaminsky, Z., Guo, X., Sharp, A. H., Amaravi, R. K., Kleiderlein, J. J., Margolis, R. L., Troncoso, J. C., Lanahan, A. A., Worley, P. F., Dawson, V. L., Dawson, T. M., and Ross, C. A. (1999) Synphilin-1 associates with alpha-synuclein and promotes the formation of cytosolic inclusions, *Nat. Genet. 22*, 110−114.
48. Conway, K. A., Harper, J. D., and Lansbury, P. T. (1998) Accelerated in vitro fibril formation by a mutant alpha-synuclein linked to early-onset Parkinson disease, *Nat. Med. 4*, 1318−1320.
49. Conway, K. A., Harper, J. D., and Lansbury, P. T., Jr. (2000) Fibrils formed in vitro from alpha-synuclein and two mutant forms linked to Parkinson's disease are typical amyloid, *Biochemistry 39*, 2552−2563.
50. Crowther, R. A., Jakes, R., Spillantini, M. G., and Goedert, M. (1998) Synthetic filaments assembled from C-terminally truncated alpha-synuclein, *FEBS Lett. 436*, 309−312.
51. El-Agnaf, O. M., Jakes, R., Curran, M. D., and Wallace, A. (1998) Effects of the mutations Ala30 to Pro and Ala53 to Thr on the physical and morphological properties of alpha-synuclein protein implicated in Parkinson's disease, *FEBS Lett. 440*, 67−70.
52. Hashimoto, M., Hsu, L. J., Sisk, A., Xia, Y., Takeda, A., Sundsmo, M., and Masliah, E. (1998) Human recombinant NACP/alpha-synuclein is aggregated and fibrillated in vitro: relevance for Lewy body disease, *Brain Res. 799*, 301−306.
53. Giasson, B. I., Uryu, K., Trojanowski, J. Q., and Lee, V. M. (1999) Mutant and wild-type human alpha-synucleins assemble into elongated filaments with distinct morphologies in vitro, *J. Biol. Chem. 274*, 7619−7622.
54. Narhi, L., Wood, S. J., Steavenson, S., Jiang, Y., Wu, G. M., Anafi, D., Kaufman, S. A., Martin, F., Sitney, K., Denis, P., Louis, J. C., Wypych, J., Biere, A. L., and Citron, M. (1999) Both familial Parkinson's disease mutations accelerate alpha-synuclein aggregation, *J. Biol. Chem. 274*, 9843−9846.
55. Serpell, L. C., Berriman, J., Jakes, R., Goedert, M., and Crowther, R. A. (2000) Fiber diffraction of synthetic alpha-synuclein filaments shows amyloid-like cross-beta conformation, *Proc. Natl. Acad. Sci. U.S.A. 97*, 4897−4902.
56. Biere, A. L., Wood, S. J., Wypych, J., Steavenson, S., Jiang, Y., Anafi, D., Jacobsen, F. W., Jarosinski, M. A., Wu, G. M., Louis, J. C., Martin, F., Narhi, L. O., and Citron, M. (2000) Parkinson's disease-associated alpha-synuclein is more fibrillogenic than beta- and gamma-synuclein and cannot cross-seed its homologues, *J. Biol. Chem. 275*, 34574−34579.
57. Uversky, V. N., Li, J., and Fink, A. L. (2001) Evidence for a partially folded intermediate in α-synuclein fibril formation, *J. Biol. Chem. 276*, 10737−10744.
58. Conway, K. A., Lee, S. J., Rochet, J. C., Ding, T. T., Williamson, R. E., and Lansbury, P. T., Jr. (2000) Acceleration of oligomerization, not fibrillization, is a shared property of both alpha-synuclein mutations linked to early-onset Parkinson's disease: implications for pathogenesis and therapy, *Proc. Natl. Acad. Sci. U.S.A. 97*, 571−576.
59. LeVine, H. D. (1993) Thioflavine T interaction with synthetic Alzheimer's disease beta-amyloid peptides: detection of amyloid aggregation in solution, *Protein Sci. 2*, 404−410.
60. Naiki, H., Higuchi, K., Hosokawa, M., and Takeda, T. (1989) Fluorometric determination of amyloid fibrils in vitro using the fluorescent dye, thioflavin T1, *Anal. Biochem. 177*, 244−249.
61. Ginsberg, S. D., Crino, P. B., Lee, V. M., Eberwine, J. H., and Trojanowski, J. Q. (1997) Sequestration of RNA in Alzheimer's disease neurofibrillary tangles and senile plaques, *Ann. Neurol. 41*, 200−209.
62. Ginsberg, S. D., Galvin, J. E., Chiu, T. S., Lee, V. M., Masliah, E., and Trojanowski, J. Q. (1998) RNA sequestration to pathological lesions of neurodegenerative diseases, *Acta Neuropathol. (Berlin) 96*, 487−494.
63. Cardin, A. D., and Weintraub, H. J. (1989) Molecular modeling of protein-glycosaminoglycan interactions, *Arteriosclerosis 9*, 21−32.

64. Cardin, A. D., and Jackson, R. L. (1988) Structural properties of the heparin-binding domains of human apolipoprotein E, *Adv. Exp. Med. Biol. 243*, 157−163.
65. Stone, A. L. (1977) Optical conformation of heparin and heparin complexes with cationic dyes, amines and protein models, *Fed. Proc. 36*, 1−16.
66. Ueda, K., Fukushima, H., Masliah, E., Xia, Y., Iwai, A., Yoshimoto, M., Otero, D. A., Kondo, J., Ihara, Y., and Saitoh, T. (1993) Molecular cloning of cDNA encoding an unrecognized component of amyloid in Alzheimer disease, *Proc. Natl. Acad. Sci. U.S.A. 90*, 11282−11286.
67. Jakes, R., Spillantini, M. G., and Goedert, M. (1994) Identification of two distinct synucleins from human brain, *FEBS Lett. 345*, 27−32.
68. Rochet, J. C., Conway, K. A., and Lansbury, P. T., Jr. (2000) Inhibition of fibrillization and accumulation of prefibrillar oligomers in mixtures of human and mouse alpha-synuclein, *Biochemistry 39*, 10619−10626.
69. Wood, S. J., Wypych, J., Steavenson, S., Louis, J. C., Citron, M., and Biere, A. L. (1999) alpha-synuclein fibrillogenesis is nucleation-dependent. Implications for the pathogenesis of Parkinson's disease, *J. Biol. Chem. 274*, 19509−19512.
70. Atoji, Y., Yamamoto, Y., and Suzuki, Y. (1995) The presence of chondroitin sulfate A and C within axon terminals in the superior olivary nuclei of the adult dog, *Neurosci. Lett. 189*, 39−42.
71. Li, J., Uversky, V. N., and Fink, A. L. (2001) Effect of Familial Parkinson's Disease Point Mutations A30P and A53T on the Structural Properties, Aggregation and Fibrillation of Human α-synuclein, *Biochemistry 40*, 11604−11613.

BI011711S